

7T Human Spine Arrays with Adjustable Inductive Decoupling

B. Wu¹, C. Wang¹, R. Krug¹, D. Kelley², D. Xu¹, S. Banerjee¹, D. Vigneron^{1,3}, S. Nelson^{1,3}, S. Majumder^{1,3}, and X. Zhang^{1,3}

¹Radiology&Biomedical Imaging, University of California, San Francisco, San Francisco, CA, United States, ²GE Healthcare, San Francisco, CA, United States, ³UCSF/UC Berkeley Joint Group Program in Bioengineering, San Francisco&Berkeley, CA, United States

Introduction Ultrahigh field parallel imaging at 7T has been proven to be a promising imaging modality for humans because it can provide high spatial and temporal resolution simultaneously [1-4]. However, one of technical challenges in implementing ultrahigh field parallel imaging is to design the required transceiver arrays, especially the large size arrays, for signal excitation and reception [4]. Due to their high operating frequency and multiple-resonator structure, ultrahigh field transceiver arrays for human imaging encounter difficulties in decoupling the resonant elements, attaining sufficient B1 penetration, and even in achieving the required high operating frequency. In this work, we explore the feasibility of designing transceiver arrays for human spine parallel MR imaging at 7T using loop-type microstrip elements with proposed adjustable inductive decoupling. Preliminary 7T spine images acquired from healthy volunteers using the proposed transceiver arrays are presented.

Methods Transceiver arrays based on non-overlapped microstrip loop resonators were built for human spine imaging at 7T. Decoupling for such arrays is always critical. Several decoupling methods by using capacitors and inductors (Fig 1) were tested and compared. Fig 1a shows the commonly used capacitive decoupling [5]. This method is easy to utilize but the decoupling capacitance is sometimes impractically small at ultrahigh fields and also very sensitive to loadings [6]. Inductive decoupling (Fig 1b) is independent from resonance frequency but is not convenient by tuning an inductor to achieve optimized decoupling with different loading. Here we use an adjustable inductive decoupling shown in Fig 1c. Compared with the conventional inductive decoupling scheme, interconnecting inductors L_d have fixed value. The decoupling was easy to achieve by tuning the capacitors C_d and/or C_i . This can be expressed by Eq. 1 shown below, where L is inductance of each loop, m is coupling coefficient (which is the ratio of mutual inductance M to L , i.e., M/L) [6].

$$L_d = L \cdot \frac{(C_t / C_d)^2 (1 - m^2) + 2(C_t / C_d) m (1 - m)}{m(1 + C_t / C_d)^2} \quad (1)$$

Based on Eq 1, the relationship between inductor L_d and C_i/C_d with different m from 0.1 to 0.2 is plotted in Fig 3. For the inductance of L_d , 1 μ H or less is usually a practical number in such coil designs.

To investigate B1 penetration and acquisition reduction capability under a sufficient imaging coverage, two spine arrays with the same length (~50cm) were built. One has six elements (Fig 2 left) with dimensions of 6cm x 10cm for each loop. Another has four elements (Fig 2 right) with bigger loop size of 12cm x 12cm. The arrays were all built on 1.2cm thick Teflon boards with a permittivity of ~2.1. The loops are closely placed with a 1cm gap between elements. The spine transceiver arrays were tested and evaluated on bench and also on a GE 7T whole body MR scanner.

Results Scattering coefficients S11 and S21 measurements were taken on a network analyzer to evaluate the performance of the arrays. Bench test result was shown in Fig 4. Unloaded Q of the coil is around 180, Loaded Q-factor is 15~20. Each element was tuned to 298 MHz, and matched to system 50 Ohm in fully loaded case. At 7T where the overall noise is usually dominated by the sample, the losses caused by interconnecting inductors may be negligible in this case. Decoupling measured -15 ~ -20dB between the nearest neighbors. The B1 penetration of the designed 6- and 4- element arrays was evaluated using in vivo MR images acquired from healthy volunteers. Measurements showed the 4-element array had a deeper penetration of ~12cm while the 6-element array had ~9cm which may show limitations in intervertebral disc imaging unless higher transmit power or a volume transmit coil is used. GRE sub-images in fig 5 (a-d) illustrate the good coil isolation, and combined image (e) illustrates good homogeneity at spinal disc area. Fig 6 shows the sagittal image of lumbar spine (Fig.6a, GRE flip angle 30°, 256*256, slice thickness 4mm, TE/TR 3.7/150ms, NEX 10) and thoracic spine (fig.6b: FSPGR, Flip angle 20°, 256*256, slice thickness 5mm, TE/TR 2.1/120ms, NEX 1). Axial image is shown in c (GRE Flip angle 20, 256*256, Slice Thickness 5mm, TE/TR 4.2/117, FOV 20*20cm), in which spinal cord is clearly visible.

Conclusions Spine transceiver arrays at 7T are designed and constructed. Preliminary in vivo imaging of the spine was demonstrated. The microstrip loop design associated with the extra adjustable inductive decoupling is suitable for human spine imaging with large image coverage and B1 penetration. The future work will be focused on parallel excitation and investigation of the transmit efficiency of the proposed design.

Acknowledgments This work was supported in part by NIH grant EB004453, AG017762, EB007588, and ITL-Bio04-10148 and QB3 opportunity award.

References [1]. G. Adriany, et al. MRM 2005;53:433-445 [2]. C.J. Snyder et al. ISMRM 15 (2007), pp164 [3].S. Banerjee et al. MRM 2007;59:655-660 [4]. L. Carvajal, et al. ISMRM 15 (2007) pp1042 [5]. J. Lian et al. U.S Patent 5,804,969 (1998) [6]. B. Wu, et al. Conc. Magn. Reson. 31B(2) 116-126(2007)

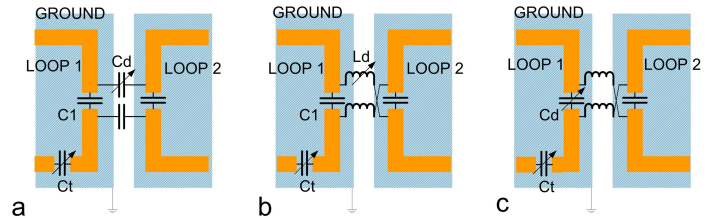


Fig 1. Decoupling method with capacitors (A), inductors (B) and adjustable inductive decoupling (C)

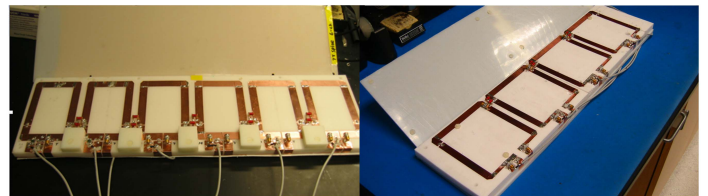


Fig 2. Six-channel and four-channel spine array with inductors for decoupling

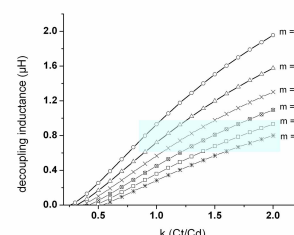


Fig 3. Decoupling condition

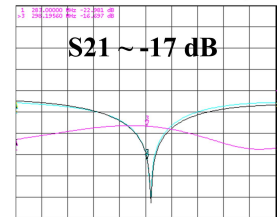


Fig 4. S parameters for inductive decoupling.

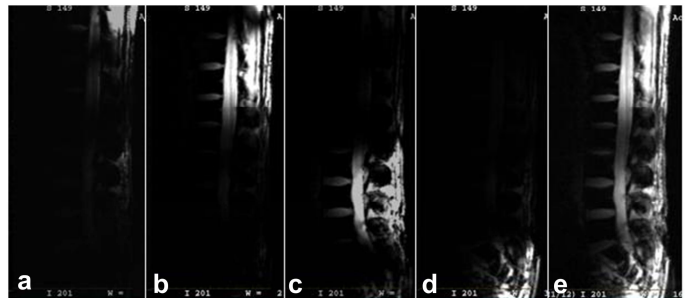


Fig 5. GRE sub-images from each coil element (a-d) and their combination (e).



Fig 6. Lumbar spine (a), thoracic spine (b) and (c).